A Highly Decoupled 8 Channel Transmit-Receive Loop Array for 7T with Diverse B1 Profiles

Graham Charles Wiggins[1], Bei Zhang[1], Gang Chen[2], and Daniel Sodickson[1]

[1]*The Bernard and Irene Schwartz Center for Biomedical Imaging, NYU Medical Center, New York, NY, United States,* [2]*The Sackler Institute of Graduate Biomedical Science, NYU School of Medicine, New York, NY, United States*

Introduction: Transmit array coils are an essential tool for parallel transmission at high field. In a typical encircling array, neighboring elements can be decoupled by various means, but it is more difficult to mitigate the often substantial coupling between next nearest neighbor coils. Many existing designs reduce this coupling through the use of shielded elements such as striplines or shielded loops, or reduce the size of the individual elements, but both strategies have the side effect of decreasing the transmit efficiency of the elements compared to a conventional surface coil loop. We describe an 8 channel Transmit-Receive (TxRx) array consisting of triangular elements which allow for capacitive decoupling of neighbors, and inductive decoupling of next nearest neighbors, resulting in a highly decoupled array which retains the transmit efficiency of a large surface coil loop element.

Methods: For comparison, 3 coils were built on identical cylindrical formers 15.24cm in diameter. The conductive structures were machined from FR4 circuit board, with all conductors of 1cm width. The length of the each coil was 12.5cm. A phantom was constructed with an inner diameter of 6cm and length of 24cm consisting of corn syrup, distilled water and salt with $\varepsilon_r = 57.5$ and $\sigma = 0.8$ to mimic average tissue properties at 297 MHz. The first coil was a high pass birdcage with four port drive (Fig. 1a). The second coil was an array of 8 rectangular surface coils which were capacitively decoupled from their neighbors via their shared edges (Fig. 1b). The third coil consisted of 8 triangular elements which were capacitively decoupled from their neighbors and also inductively decoupled from their next nearest neighbors. The two surface coil arrays were matched to 50 Ω coax by attaching the ground and signal lines of the coax to either side of a capacitor in the surface coil loop. The birdcage required a series inductor and parallel capacitor to match to the coax (Fig. 1a). A coaxial trap was placed next to each match circuit to minimize common mode currents on the cables. For the coils with match circuits at both ends, the coax was routed back across the coil through an additional trap (Fig. 2)

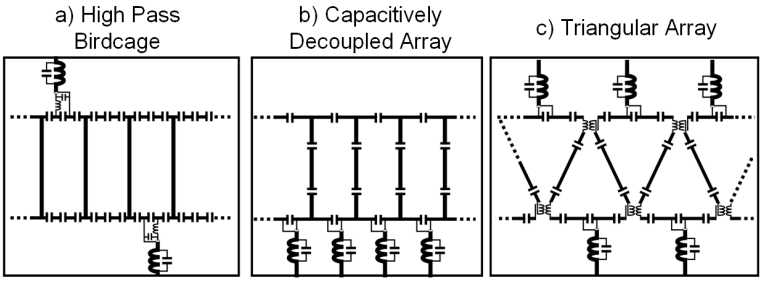

Figure 1: Circuit diagrams of three coil designs

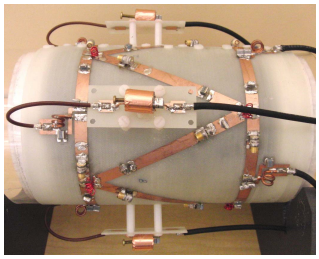

Figure 2: Triangular array

The birdcage was driven with an in-house built 4 channel power splitter, T/R switch and preamp interface, with appropriate phases applied to the ports through the control of cable length. Signals from all four ports were recorded, reconstructed and combined in Root Sum of Squares (RSS) combination. For the 8 channel arrays, power was divided with an 8 way splitter (Werlatone Patterson NY) and the coil was connected to the scanner with an in-house built 8 channel T/R switch and preamp interface. Signals from all 8 ports were recorded and combined as above. All data were acquired on a Siemens 7T scanner (Siemens Healthcare, Erlangen, Germany).

To determine the RF voltage needed to achieve a 90 degree flip angle in the center of the phantom, a turbo-FLASH sequence with various preparation pulses was used [1]. The B1+ distribution was mapped with a similar method using a manufacturer works-in-progress sequence (Siemens Healthcare, Erlangen, Germany) [2]. SNR was measured using a gradient echo acquisitions both with and without RF excitation and calculated according to the "Kellman" method [3]. G-factor maps were derived from the same gradient echo sequence but with field of view set tight on the phantom to maximize aliasing.

Results: The phantom, which nearly filled the volume of the coil, presented a very heavy load. This made it difficult to match and decouple the ports of the birdcage since the coil was overdamped. Using 4 ports (2 on each end ring) it was possible to force a symmetrical excitation, but coupling between the ports was high (-11dB). Q_{UL}/Q_L was 10 for the capacitively decoupled array (CDA) and 5.7 for the triangle array. For the CDA, coupling between next nearest neighbors was -11.6 dB when they were the only two coils active. It proved difficult to decouple neighboring coils through adjustment of the capacitors in their shared legs, but looking at 2 coils in isolation it was possible to achieve isolation of -15 dB. When all coils were made active, however, the distribution of coupling changed, with much less coupling between next nearest neighbors (~-20 dB) and higher coupling between neighbors (~ -12 dB), summarized in Figure 3a. Also apparent in Fig. 3a is high coupling between coils on opposite sides of the phantom. In contrast the triangular array was very straightforward to decouple since once a coil was decoupled from its neighbors and its next nearest neighbors it was unaffected by any changes to the rest of the array. Coupling between elements was -20 dB or less for all coil pairs (Fig. 3b).

The birdcage, CDA and triangle array the scanner transmitter reference voltages were 119, 106 and 100 volts respectively. The overall excitation pattern (not shown) is very similar for each coil, apart from drop-outs due to coupling in the birdcage and a bias towards the driving end of the CDA. SNR plots are shown in Figure 4. Both 8 channel arrays achieve comparable SNR, with the CDA having higher SNR in the periphery. The birdcage central SNR is not too different from the other coils, but drops off towards the periphery as we would expect. The triangular coil shows performance advantages, however, when we look at g-factor maps (Figure 6). G-factor values in an axial plane are very similar for the two coils, but attempting to accelerate along Z with a coronal slice causes huge noise amplification with the CDA since the elements have no variation in that direction. The alternating triangular elements provide encoding along Z for both reception and transmission. Example B1+ maps for individual elements are shown in Figure 6, where it can be seen that Coil 1 and Coil 2 swap intensity as you move along Z for the triangle coil but not for the CDA

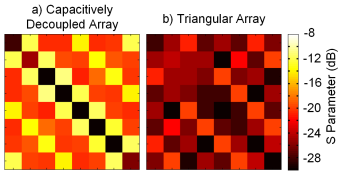

Figure 3: Coupling matrices (S_{21}) for the two 8 element arrays. Values on the diagonal are S_{11} reflection for each element

Conclusions: The triangle array design allows for explicit decoupling of 1st and 2nd order neighbors, creating a highly decoupled array. With less power coupled to other ports it is more efficient, and the B1 variation along Z allows for acceleration along Z for parallel transmit or receive.

[1] Breton E. NMR Biomed. 2010 May;23(4):368-74 [2] Klose U, Med. Phys. 19 (4), 1992 [3] Kellman P. MRM 54:1439–1447 (2005)

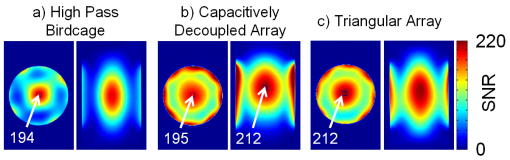

Figure 4: SNR plots for root sum of squares reconstruction for the 3 coil designs

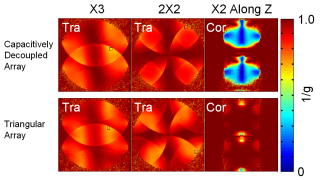

Figure 5: Plots of 1/g-factor for the two 8 channel coils

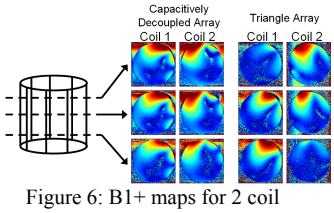

Figure 6: B1+ maps for 2 coil elements as function of Z position